

**Serveur Académique Lausannois SERVAL [serval.unil.ch](http://serval.unil.ch)**

## **Author Manuscript**

**Faculty of Biology and Medicine Publication**

**This paper has been peer-reviewed but does not include the final publisher proof-corrections or journal pagination.**

Published in final edited form as:

**Title:** Contribution of Intronic miR-338-3p and Its Hosting Gene AATK to Compensatory  $\beta$ -Cell Mass Expansion.

**Authors:** Jacovetti C, Jimenez V, Ayuso E, Laybutt R, Peyot ML, Prentki M, Bosch F, Regazzi R

**Journal:** Molecular endocrinology (Baltimore, Md.)

**Year:** 2015 May

**Volume:** 29

**Issue:** 5

**Pages:** 693-702

**DOI:** 10.1210/me.2014-1299

In the absence of a copyright statement, users should assume that standard copyright protection applies, unless the article contains an explicit statement to the contrary. In case of doubt, contact the journal publisher to verify the copyright status of an article.

1           **Contribution of intronic miR-338-3p and its Hosting Gene AATK to**  
2                                   **Compensatory  $\beta$ -cell Mass Expansion**

3           Cécile Jacovetti<sup>1</sup>, Veronica Jimenez<sup>2</sup>, Eduard Ayuso<sup>2#</sup>, Ross Laybutt<sup>3</sup>, Marie-Line Peyot<sup>4</sup>, Marc  
4                                   Prentki<sup>4</sup>, Fatima Bosch<sup>2</sup> and Romano Regazzi<sup>1</sup>

5           <sup>1</sup>Department of Fundamental Neurosciences, University of Lausanne, Lausanne, Switzerland.

6           <sup>2</sup>Center of Animal Biotechnology and Gene Therapy and Department of Biochemistry and Molecular  
7           Biology, School of Veterinary Medicine, Universitat Autònoma de Barcelona, Bellaterra, Centro de  
8           Investigación Biomédica en Red de Diabetes y Enfermedades Metabólicas Asociadas, Barcelona,  
9           Spain.

10          <sup>3</sup>Diabetes and Obesity Research Program, Garvan Institute of Medical Research, St. Vincent's  
11          Hospital, Sydney, New South Wales, Australia.

12          <sup>4</sup>Montreal Diabetes Research Center and CRCHUM, Montreal, QC, Canada and Departments of  
13          Nutrition, Biochemistry and Molecular Medicine, University of Montreal, QC, Canada.

14          # Present address: INSERM UMR1089, CHU de Nantes, France and Atlantic Gene Therapies, Nantes,  
15          France

16          **Abbreviated title:** Role of miR-338-3p and AATK in  $\beta$ -cell Expansion

17          **Key terms:** Intronic miR-338-3p; host gene AATK; pancreatic  $\beta$ -cell proliferation

18          **Word count:** 4266 words

19          **Number of figures and tables:** 6

20          **Corresponding author and person to whom reprint requests should be addressed:**

21          Dr. Romano Regazzi, Department of Fundamental Neurosciences

22          Rue du Bugnon 9, CH-1005 Lausanne, Switzerland

23          Tel. : +41 21 692 52 80 / Fax : +41 21 692 52 55

24          E-mail : [Romano.Regazzi@unil.ch](mailto:Romano.Regazzi@unil.ch)

25  
26          **Disclosure statement:** The authors have nothing to disclose.

## 27 **Abstract**

28 The elucidation of the mechanisms directing  $\beta$ -cell mass regeneration and maintenance is of interest  
29 since the deficit of  $\beta$ -cell mass contributes to diabetes onset and progression. We previously found that  
30 the level of the microRNA miR-338-3p is decreased in pancreatic islets from rodent models displaying  
31 insulin resistance and compensatory  $\beta$ -cell mass expansion, including pregnant rats, diet-induced  
32 obese mice and *db/db* mice. Transfection of rat islet cells with oligonucleotides that specifically block  
33 miR-338-3p activity increased the fraction of proliferating  $\beta$ -cells *in vitro* and promoted survival under  
34 pro-apoptotic conditions without affecting the capacity of  $\beta$ -cells to release insulin in response to  
35 glucose. Here, we evaluated the role of miR-338-3p *in vivo* by injecting mice with an Adeno-  
36 Associated viral (AAV) vector permitting specific sequestration of this microRNA in  $\beta$ -cells. We  
37 found that the AAV construct increased the fraction of proliferating  $\beta$ -cells confirming the data  
38 obtained *in vitro*. miR-338-3p is generated from an intron of the gene coding for Apoptosis-Associated  
39 Tyrosine Kinase (AATK). Similarly to miR-338-3p, we found that AATK is down-regulated in rat and  
40 human islets and INS832/13  $\beta$ -cells in the presence of the cAMP-raising agents exendin-4, estradiol  
41 and a GPR30 agonist. Moreover, AATK expression is reduced in islets of insulin resistant animal  
42 models and selective silencing of AATK in INS832/13 cells by RNA interference promoted  $\beta$ -cell  
43 proliferation. The results point to a coordinated reduction of miR-338-3p and AATK under insulin  
44 resistance conditions and provide evidence for a cooperative action of the microRNA and its hosting  
45 gene in compensatory  $\beta$ -cell mass expansion.

## 46 **Introduction**

47 MicroRNAs (miRNAs) form a large family of short ( $\approx 22$ nt) single-stranded non-coding RNAs which  
48 are critical posttranscriptional regulators of gene expression (1,2). These small RNA molecules  
49 function by partially pairing to the 3' untranslated region (UTR) of target mRNAs thereby inhibiting  
50 their translation and/or stability. Numerous miRNAs have been shown to play major roles in the  
51 regulation of  $\beta$ -cell functions, including insulin secretion, proliferation and survival (3,4). Mammalian  
52 miRNAs are generated from diverse genomic locations and can be either intergenic and transcribed  
53 from their own independent unit or intronic and transcribed from introns of protein-coding genes or  
54 from introns of non-coding genes (5,6). Some intronic miRNAs are co-regulated with their hosting  
55 genes and have analogous functions, whereas others display opposite expression profiles and have  
56 antagonistic roles (7). Bioinformatic studies revealed that about one third of the intronic miRNAs  
57 possess their own promoters, while the others are co-transcribed with their hosting genes and are  
58 processed from the same primary transcript (8,9).

59 Recently, we showed that miR-338-3p is down-regulated in islets under conditions of insulin  
60 resistance, such as pregnancy and obesity, and upon exposure of  $\beta$ -cells to 17- $\beta$  estradiol and to the  
61 GLP1-analogue exendin-4. We also observed that blockade of miR-338-3p *in vitro* and in transplanted  
62 islets leads to increased  $\beta$ -cell proliferation and improved survival under pro-apoptotic conditions (10).  
63 However, the beneficial impact of reduced miR-338-3p activity on  $\beta$ -cell function *in vivo* remained to  
64 be proven. This particular miRNA is generated from the seventh intron of the Apoptosis-Associated  
65 Tyrosine Kinase (AATK) gene, also called Lemur Kinase 1 (LMTK1) (5). Recent studies in other cell  
66 systems have evidenced a co-regulation of miR-338-3p and its hosting gene, and this miRNA was  
67 proposed to serve the interest of AATK by silencing several genes that act antagonistically to AATK  
68 (11). Although, AATK has been shown to play a role in cell differentiation, growth and apoptosis (12-  
69 17) its biological relevance in insulin-producing cells is unknown.

70 The objective of our study was first to verify whether the proliferative effect of miR-338-3p observed  
71 *in vitro* is conserved *in vivo* and second, to determine whether the hosting gene AATK synergizes or  
72 antagonizes the action of the miRNA.

73 **Materials and methods**

74

75 **Chemicals**

76 TNF $\alpha$  and IFN $\gamma$  were from R&D Systems. IL-1 $\beta$ , Tnfrsf1b, exendin-4, 17- $\beta$  estradiol, 3-Isobutyl-1-  
77 methylxanthine (IBMX) and G1 were obtained from Sigma-Aldrich.

78

79 **Animals**

80 Male and pregnant Wistar rats were obtained from Charles River laboratories and were housed on a  
81 12:12 h light-dark cycle in climate-controlled and pathogen-free facilities. 8-week-old male ICR mice  
82 were used to inject AAV8 intraductally. All procedures were performed in accordance with the  
83 National Institutes of Health guidelines, and were approved by the Swiss Research Councils and  
84 Veterinary Office and by the Ethics Committee in Animal and Human Experimentation of the  
85 Universitat Autònoma de Barcelona. Four week-old male C57BL/6 mice were purchased from Charles  
86 River Laboratories (Saint-Constant, QC, Canada) and fed a normal diet or HFD (Bio-Ser Diet number  
87 F3282, Frenchtown, NJ, USA; 60% [wt/wt] energy from fat) for 8 weeks. The detailed sources of  
88 *db/db* and diet-induced obese mice have been described previously (18,19).

89

90 **Isolation and culture of islet cells**

91 Pancreatic islets were isolated as described (20) by collagenase digestion followed by purification on a  
92 Histopaque (Sigma-Aldrich) density gradient. The islets were first cultured overnight in RPMI 1640  
93 Glutamax medium (Invitrogen) supplemented with 10% fetal calf serum (FCS; Amimed), 50 U/ml  
94 penicillin, 50ug/ml streptomycin, 1 mmol/l Na Pyruvate and 250  $\mu$ mol/l Hepes. Human islets were  
95 obtained from the Cell Isolation and Transplantation Center from the University of Geneva, through  
96 the ECIT "Islets for Research" distribution program supported by the Juvenile Diabetes Research  
97 Foundation. The use of human islets was approved by the Geneva institutional ethical committee.  
98 After isolation, the islets were kept in culture for one or two days before treatment. Whole human  
99 islets were cultured in CMRL medium (Invitrogen) supplemented with 10% FCS, 100 U/ml penicillin,

100 100µg/ml streptomycin, 2mmol/l glutamine and 250 µmol/l Hepes. Detailed information about the  
101 human islet preparations used in this study is presented in the Supplemental Table 3.

102

### 103 **Transfection and modulation of miR-338-3p and AATK levels**

104 INS832/13 cells or MIN6B1 cells were transfected using Lipofectamine 2000<sup>TM</sup> (Invitrogen) with  
105 single-stranded miScript miRNA inhibitors (Qiagen) that specifically block endogenous miR-338-3p  
106 or with the miScript miRNA reference inhibitor (Qiagen) as a negative control. To modulate the level  
107 of the hosting gene, the cells were transfected with a small interfering RNA (siRNA) duplex against  
108 AATK or with a custom-designed siRNA duplex against green fluorescent protein that was used as  
109 negative control. To experimentally sequester and inhibit the activity of miR-338-3p, MIN6B1 cells  
110 were transfected for three days with plasmids expressing enhanced green fluorescent protein (EGFP)-  
111 labelled constructs driven by the Rat Insulin Promoter II (RIP-II) containing either a control sponge or  
112 the miR-338-3p sponge.

113

### 114 **Measurement of miRNA and mRNA expression**

115 Mature miRNA expression was assessed by qRT-PCR using the miRCURY LNA<sup>TM</sup> Universal RT  
116 microRNA PCR kit (Exiqon). miRNA primers were purchased from Exiqon. Messenger RNA  
117 expression was measured by conventional reverse transcription (Promega) followed by qRT-PCR  
118 (Biorad) with custom-designed primers (Microsynth). Primer sequences are available on request.  
119 miRNA expression was normalized to the level of U6 small nuclear ribonucleoprotein. mRNA  
120 expression was normalized to the amount of 18S present in the same samples.

121

### 122 **Insulin secretion**

123 Three days after transfection, INS832/13 cells were pre-incubated during 30 minutes at 37°C in Krebs-  
124 Ringer buffer (25 mM HEPES, pH 7.4, 127 mM NaCl, 4.7 mM KCl, 1 mM CaCl<sub>2</sub>, 1.2 mM KH<sub>2</sub>PO<sub>4</sub>,  
125 1.2 mM MgSO<sub>4</sub> and 5 mM NaHCO<sub>3</sub>) containing 2 mmol/l glucose. The pre-incubation medium was  
126 discarded and the cells incubated for 45 minutes in the same buffer (basal condition) or with Krebs-  
127 Ringer buffer containing 20 mmol/l glucose, 10 µM Forskolin and 100 µM IBMX (stimulatory

128 condition). At the end of the incubation period, the medium was collected and total cellular insulin  
129 contents recovered with ethanol acid (75% ethanol, 0.55% HCl). The amount of insulin in the samples  
130 was determined using an insulin enzyme immunoassay kit (ELISA, Mercodia).

131

### 132 **Cell death assessment**

133 Three days after transfection, transfected INS832/13 or MIN6B1 cells were incubated with 1 µg/ml  
134 Hoechst 33342 (Invitrogen) during 1 minute. The fraction of cells displaying picnotic nuclei was  
135 scored under fluorescence microscopy (AxioCam MRc5, Zeiss). Apoptosis was triggered by exposing  
136 the cells during 24h to cytokines (10 ng/ml TNF $\alpha$ , 0.1 ng/ml IL-1 $\beta$  and 30 mg/ml IFN $\gamma$ ) or during 48h  
137 to culture medium containing 5% FCS and supplemented with 0.5 mmol/l palmitate bound to 0.5%  
138 BSA.

139

### 140 **Proliferation assay**

141 Three days after transfection, transfected INS832/13 or MIN6B1 cells and rat islet cells cultured on  
142 Poly-L-lysine coated glass coverslips, were fixed with ice-cold methanol and permeabilized with 0.5%  
143 saponin (Sigma-Aldrich). The coverslips were incubated with a rabbit anti-Ki67 antibody (ab66155  
144 Abcam) at 1:1500 and then with goat anti-rabbit Alexa Fluor 488 (A11008 Invitrogen). Pictures were  
145 collected using a fluorescence microscope (AxioCam MRc5, Zeiss).

146

### 147 **Protein extraction and western Blotting**

148 Proteins lysates (30-50 µg) from INS832/13 cells were separated on polyacrylamide gels and  
149 transferred to nitrocellulose membranes. The membranes were incubated overnight at 4°C with  
150 primary antibody against AATK (Ab100587 Abcam; 1:500), AKT (Cell Signaling #2920; 1:500),  
151 phospho-AKT (Cell Signaling #9275; 1:500) or against  $\alpha$ -Tubulin (T9026 Sigma Aldrich, 1:10000).  
152 After one hour exposure to IRDye (Li-Cor® Biosciences), the bands were visualized via the Odyssey  
153 imaging system (Li-Cor® Biosciences). Band intensity was quantified by using ImageJ software.

154

155



156

### 157 **Recombinant AAV vectors**

158 Single-stranded AAV vectors of serotype 8 were generated by triple transfection of human embryonic  
159 kidney 293 cells and purified by the CsCl-based gradient method (21). Transgenes used expressed a  
160 construct coding for EGFP driven by the rat insulin promoter II (RIP-II) and carried either a sponge  
161 against miR-338-3p or against a scrambled sequence. Purified AAV vectors were dialyzed against  
162 PBS, filtered and stored at -80°C. Titers of viral genomes (vg) were determined by qRT-PCR as  
163 described (22).

164

### 165 **Administration of AAV vectors**

166 Retrograde pancreatic intraductal injections were performed as described previously (23). Mice were  
167 anesthetized with ketamine (100 mg/kg) and xylazine (10 mg/kg). A dose of  $10^{12}$  vg/mouse (100  $\mu$ L  
168 AAV solution/mouse) was intraductally administered.

169

### 170 **Luciferase assays**

171 A miR-338-3p sensor plasmid was generated by cloning a sequence complementary to the miRNA  
172 between the EcoR1 and XhoI restriction sites of psiCHECK-1 (Promega). An analogous approach was  
173 used to generate the plasmid including the 3'UTR of rat Tnfrsf1b containing the putative binding site  
174 of miR-338-3p. Luciferase activity was measured in INS832/13 or MIN6B1 cells with a dual-  
175 luciferase reporter assay (Promega, Madison, WI) three days after transfection. Renilla luciferase  
176 activity was normalized for transfection efficiency to the SV40-driven Firefly activity generated by the  
177 PGL3 promoter vector (Promega).

178

### 179 **Immunohistochemistry**

180 Tissues were fixed for three days in 10% formalin, embedded in paraffin and sectioned. The pancreatic  
181 slices were then incubated overnight at 4°C with the following antibodies: 1:300 goat anti-GFP  
182 (ab6673 Abcam), 1:200 guinea pig anti-insulin (ab7842 Abcam) or 1:300 rabbit anti-Ki67 (ab66155  
183 Abcam). As secondary antibodies, biotinylated donkey anti-goat (sc-2042 Santa Cruz), streptavidin

184 Alexa Fluor 488 (S-11223 Molecular Probes), goat anti-guinea pig Alexa Fluor 555 (A21435  
185 Invitrogen), goat anti-rabbit Alexa Fluor 555 (A21428 Invitrogen) at 1:300 were used. Sections were  
186 counterstained with Hoechst 33342 (Invitrogen) for nuclear labeling. A Zeiss Axiovision fluorescence  
187 microscope was used. For measurement of  $\beta$ -cell proliferation, three pancreatic slices (200  $\mu$ m apart)  
188 were stained with anti-Ki67 and anti-GFP antibodies, and nuclei were counterstained with Hoechst.  
189 Replicative cells were identified by double Ki67 and GFP immunostaining. The  $\beta$ -cell mass was  
190 calculated by multiplying pancreas weight by percentage of  $\beta$ -cell area. The percentage of  $\beta$ -cell area  
191 per pancreas was analyzed in three insulin-stained sections 200  $\mu$ m apart, by dividing the area of all  
192 insulin positive cells in one section by the total area of that section. An islet was considered as infected  
193 by the viruses if at least one insulin-positive cell was also positive for EGFP.

194

#### 195 **Statistical analysis**

196 Statistical differences were tested using a Student's t-test or, for multiple comparisons, with ANOVA  
197 followed by a post-doc Dunnett test, with a discriminating p value of 0.05 (SAS statistical package).

## 198 **Results**

### 199 **$\beta$ -cell specific inhibition of miR-338-3p promotes cell proliferation *in vivo***

200 To inhibit the activity of miR-338-3p *in vivo*, we engineered a “microRNA sponge” (24,25) capable of  
201 specifically inhibiting the activity of this miRNA in  $\beta$ -cells. Our construct is driven by the rat insulin  
202 promoter and contains the coding region of EGFP with 7 binding sites for miR-338-3p in the 3’UTR.  
203 By capturing miR-338-3p, the sponge prevents the interaction with the endogenous targets of the  
204 miRNA (Figure 1A). Indeed, the transfection of the miR-338-3p sponge in the insulin-secreting cell  
205 line MIN6B1 led to an increase in the expression of a luciferase reporter construct containing the  
206 binding site of the miRNA (Supplemental Fig. 1A) and reproduced the functional effects of anti-miR-  
207 338-3p (10) resulting in an increased proliferation rate and enhanced survival under pro-apoptotic  
208 conditions (Supplemental Fig. 1B, C). To examine whether inhibition of miR-338-3p activity *in vivo*  
209 promotes the replication of  $\beta$ -cells, a dose of  $1 \times 10^{12}$  viral genomes/mouse of AAV8 vectors carrying  
210 the RIP-II-GFP-miR-338-3p sponge cassette or RIP-II-GFP-control sponge were injected into the  
211 pancreatic duct of adult ICR mice. One month after AAV administration, immunostaining revealed  
212 that more than 80% of the islets were transduced by these AAV8 vectors and expressed the construct  
213 (Figure 1B). Double immunostaining for insulin and GFP confirmed that the construct was exclusively  
214 expressed in  $\beta$ -cells. Quantification of the number of GFP<sup>+</sup>  $\beta$ -cells demonstrated an average of 20%  
215 transduced  $\beta$ -cells (Figure 1C, D). The sponge was not expressed by glucagon-positive cells  
216 (Supplemental Fig. 2). The fraction of proliferating GFP<sup>+</sup>  $\beta$ -cells receiving the control sponge was  
217 identical to that of non-transduced islet cells (Figure 1E). In contrast, the GFP<sup>+</sup>  $\beta$ -cells receiving the  
218 AAV8-miR-338-3p sponge displayed a significant increase in the proliferation rate (Figure 1E, F).  
219 Consistent with these observations, the fraction of proliferating insulin-positive cells was increased in  
220 islets transduced with the miR-338-3p sponge compared to islets receiving the control sponge (Figure  
221 1G, H). One month after viral injection, no significant change in  $\beta$ -cell mass was observed between  
222 the two groups of mice (Figure 1I). Analysis of individual glycemic profiles revealed no differences  
223 between the two groups (data not shown). Overall the data demonstrate the conserved beneficial  
224 impact of reduced activity of miR-338-3p in promoting  $\beta$ -cell proliferation capacity *in vivo*.

## 225 **miR-338-3p and its hosting gene AATK are co-regulated**

226 We previously reported reduced expression of miR-338-3p in islets of insulin resistant animals  
227 displaying compensatory  $\beta$ -cell mass expansion (10). Since this miRNA is encoded within one of the  
228 introns of AATK (Supplemental Fig. 3), we analyzed in the same samples the expression of the  
229 hosting gene. Similarly to miR-338-3p, we found that AATK mRNA decreases in islets of rats during  
230 pregnancy reaching the minimal level at day 14 of gestation (corresponding to the peak of  $\beta$ -cell mass  
231 expansion) and returned close to pre-pregnancy levels 3-days post-partum (Figure 2A). AATK  
232 expression is also reduced to a similar extent than miR-338-3p in islets of two animal models  
233 characterized by insulin resistance and compensatory  $\beta$ -cell mass expansion (Supplemental Tables 1  
234 and 2): 6 week-old pre-diabetic *db/db* mice (Figure 2B) and diet-induced obese mice fed a high-fat  
235 diet for 8 weeks (Figure 2C). These results suggest a common regulation of the expression profile of  
236 the gene coding for AATK and its intronic miRNA in pancreatic islets under conditions of insulin  
237 resistance.

238 In view of these findings, to determine if miR-338-3p and AATK expression is coordinated we  
239 measured AATK mRNA levels in INS832/13 cells exposed to the cAMP-raising agent IBMX. We  
240 found that the changes in the level of miR-338-3p and AATK follow the same kinetics and are  
241 maximal after about 4 hours of treatment (Figure 3). We then exposed rat and human islets to  
242 estradiol, a hormone capable of eliciting a decrease of miR-338-3p expression by binding to its non-  
243 canonical GPR30 receptor that activates the cAMP-dependent pathway (10). We found that exposure  
244 of rat and human islets to 17- $\beta$  estradiol for 48 hours decreases the expression of AATK (Figure 4A,  
245 B). Treatment with G1, a specific GPR30 agonist, produced the same effect in rat islets (Figure 4C).  
246 GLP1 is also able to reduce the level of miR-338-3p by activating the cAMP-dependent pathway (10).  
247 In line with the effect of other hormones triggering cAMP-dependent signaling, the stable GLP1  
248 analog exendin-4 represses AATK levels both in rat and human islets (Figure 4D, E). A similar effect  
249 was also observed in INS832/13 cells both at the mRNA and at the protein level (Supplemental Fig.  
250 4).

251

## 252 **Functional roles of AATK in insulin-secreting cells**

253 In order to investigate the functional role of AATK in  $\beta$ -cells and compare it to that of miR-338-3p,  
254 we used RNA interference to silence AATK mRNA and protein levels in INS832/13 cells. The siRNA  
255 treatment, faithfully reproduced the decrease of approximately 50% of AATK mRNA observed in  
256 islets of insulin resistant animal models, without affecting the level of miR-338-3p (Figure 5A).  
257 AATK protein levels were also reduced by about half (Figure 5B, C). A specific antisense LNA-  
258 oligonucleotide (anti-miR) was also transiently transfected in INS832/13 cells to target and inhibit the  
259 endogenous miRNA without altering the mRNA level of AATK (Figure 5D). We first assessed the  
260 impact of the silencing of miR-338-3p and of its hosting gene on  $\beta$ -cell proliferation. Interestingly,  
261 inhibition of either miR-338-3p or AATK increased the proliferation of INS832/13 cells (Figure 6A)  
262 without significantly affecting insulin release (Figure 6B) and insulin content (Figure 6C). Moreover,  
263 in agreement with our previous results, the inhibition of miR-338-3p protected the cells against the  
264 toxic effects of pro-inflammatory cytokines and palmitate (Figure 6D, E). In contrast, the reduction of  
265 AATK did not promote cell survival under these pro-apoptotic conditions (Figure 6D, E).

266 The precise mechanism through which miR-338-3p affects  $\beta$ -cell proliferation and survival remains to  
267 be elucidated. Functional analysis of the potential targets revealed enrichment in genes involved in  
268 cancer development, MAP kinase pathway and cytokine signaling (Supplemental Table 4). We indeed  
269 obtained evidence indicating that miR-338-3p directly targets *Tnfrsf1b* (26), potentially explaining  
270 part of the anti-apoptotic but not of the proliferative effect of the miRNA (Supplemental Fig. 5). We  
271 previously identified several key gene expression changes elicited by miR-338-3p blockade in rat and  
272 human islets (10) that mimic the mRNA expression profile observed in islets of insulin resistant  
273 animals (10,27-30). As expected, similar modifications of genes involved in proliferation and survival  
274 (*Birc5*, *Foxm1*, *Cyclin D2*, *Igf1r*, *Irs2*, *Bcl2*, *Bcl-x1*, *Bad*) were observed upon repression of miR-338-  
275 3p in tumoral INS832/13  $\beta$ -cells (Figure 6F) and led to the activation of the AKT signaling  
276 (Supplemental Fig. 6). Consistent with its functional impact on cell proliferation, silencing of AATK  
277 in INS832/13 cells led to an increase in the expression of *Igf1r* and *Irs2*, two genes that are part of an  
278 autocrine loop involved in regulating  $\beta$ -cell proliferation (31,32) (Figure 6F). In contrast, reduced

279 levels of AATK did not trigger any modification in the expression of the anti- or pro-apoptotic genes  
280 Bcl2, Bcl-xl and Bad (Figure 6F) as miR-338-3p did. Altogether these results strongly support the  
281 hypothesis of a cooperative action of miR-338-3p and its hosting gene AATK on  $\beta$ -cell proliferation  
282 and in promoting the expansion of the functional  $\beta$ -cell mass under insulin resistant conditions.

283

## 284 **Discussion**

285 In the present study, we have identified  $\beta$ -cell specific down-regulation of miR-338-3p as a powerful  
286 strategy to promote  $\beta$ -cell proliferation *in vivo*. Furthermore, we extend our understanding of the  
287 regulation and functional role of the miR-338-3p hosting gene AATK. The results reveal a parallel  
288 down-regulation of the miRNA and its hosting gene in islets of insulin resistant animal models and in  
289 response to activation of the cAMP-dependent pathway. In addition, we were able to show that AATK  
290 contributes to the regulation of  $\beta$ -cell proliferation by activating signaling pathways that are common  
291 to those of the miRNA.

292 Conventional knock-out (KO) mouse models are often used to study the role of miRNAs *in vivo*.  
293 However, about 30-40% of known mammalian miRNAs are located within introns of protein coding  
294 genes (5,33). Thus, the phenotype of miRNA KO animals can be influenced by the simultaneous  
295 invalidation of their hosting gene (34). To circumvent this problem, strategies avoiding to manipulate  
296 the genome and permitting direct interference with the function of the mature miRNA have been  
297 developed. *In vivo* delivery of miRNA sponges constitutes an interesting approach to study miRNA  
298 loss-of-function phenotypes and is emerging as a very attractive alternative to the use of KO mouse  
299 models. miRNA sponges have been demonstrated to be powerful inhibitors of miRNA activity due to  
300 the presence of multiple binding sites that sequester their target miRNA, thus preventing the  
301 interaction with their endogenous targets (24). A major advantage of this strategy is that it permits  
302 repression of miRNA activity in adult animals, avoiding problems associated with the invalidation of  
303 the miRNA during the fetal period and possible developmental defects. An efficient strategy of  
304 miRNA sponge delivery in mouse tissues is the use of viral vectors (25). In the past decade, new AAV  
305 vectors have been engineered, providing efficient gene transfer vehicles driven by tissue-specific  
306 promoters that have the tremendous advantage of lacking pathogenicity and displaying low  
307 immunogenicity (35). Studies showed that intraductal delivery of single stranded AAV vectors permits  
308 high gene transfer efficiency in endocrine islet cells (23).

309 Here we have combined a miRNA sponge approach with an AAV delivery strategy to study miR-338-  
310 3p action *in vivo*. To our knowledge, this is the first study with AAV-mediated delivery of a miRNA  
311 sponge specifically in pancreatic  $\beta$ -cells. Our results now confirm *in vivo* the involvement of miR-338-  
312 3p in the control of  $\beta$ -cell proliferation and suggest that AAV-based delivery of miR-338-3p inhibitors  
313 in diabetic animal models may represent an attractive therapeutic approach to promote the  $\beta$ -cell  
314 expansion and restore an appropriate mass of insulin-secreting cells. Further investigations will be  
315 required to improve the efficiency of the delivery of the sponge since under our experimental  
316 condition only a fraction of the  $\beta$ -cells were transduced and this was insufficient to significantly  
317 increase the total  $\beta$ -cell mass. An additional aspect that will need to be re-evaluated is the AAV  
318 delivery approach. Intraductal injection is a rather invasive method to deliver the sponge. In the future,  
319 it will be possible that capsid modifications in the AAV particles will allow them to target the  $\beta$ -cells  
320 *in vivo* by means of less invasive strategies such as intraperitoneal or intravenous injections.

321 Intronic miRNAs are usually thought to be coordinately expressed with their hosting gene, suggesting  
322 that they are transcribed from a common precursor under the control of a single promoter (5,8).  
323 Consistent with the data of a previous study carried out in a neuroblastoma cell line, we found a  
324 parallel regulation of the expression of miR-338-3p and of its hosting gene AATK (11). Our findings  
325 suggest that the concomitant decrease of miR-338-3p and AATK in  $\beta$ -cells of animals with insulin  
326 resistance showing  $\beta$ -cell mass expansion involves the cAMP-dependent pathway. This observation is  
327 consistent with the activation of GPR30 or GLP1R signalling cascades that increase cAMP levels  
328 (36,37). The reduction of miR-338-3p and AATK levels elicited by these two hormones reproduced  
329 the changes observed in islets of pregnant and obese animals. Our results point to a common  
330 regulation of the expression of miR-338-3p and its hosting gene in pancreatic islets under insulin  
331 resistance conditions that involves at least in part the cAMP signaling. The possibility of a differential  
332 regulation of the level of the miRNA and its hosting gene under other specific conditions cannot be  
333 ruled out. This could potentially be achieved by the use of an alternative promoter permitting an  
334 independent transcription of miR-338-3p (38) or via post-transcriptional control mechanisms allowing  
335 a fine tuning of the level of the AATK mRNA and of miR-338-3p (39).



336 Thanks to its tyrosine kinase activity, AATK has been proposed to play a role in the terminal  
337 differentiation and growth of neurons as well as cell proliferation and to be involved in the apoptosis  
338 of mature neuronal and cancer cells (12-17). So far, this gene has not yet been investigated in  
339 pancreatic  $\beta$ -cells. In contrast to neuronal cells, the reduction of AATK in insulin-secreting cells did  
340 not impact on cell survival. This may be explained by the fact that, in contrast to miR-338-3p  
341 blockade, AATK knock-down does not lead to the up-regulation of the anti-apoptotic genes Bcl2 and  
342 Bcl-x1. However, silencing of AATK resulted in a significant increase of replicating  $\beta$ -cells,  
343 suggesting that its down-regulation under conditions of insulin resistance may contribute to  
344 compensatory  $\beta$ -cell mass expansion. This view is supported by the fact that both miR-338-3p and  
345 AATK down-regulation elicit  $\beta$ -cell proliferation in association with increased expression of *Igf1r* and  
346 *Igf2* genes. In fact, these two proteins are the central components of an autocrine signaling loop that  
347 controls  $\beta$ -cell mass expansion under insulin resistance conditions (31,32). None of the genes  
348 differentially expressed in the presence of the anti-miRNA are predicted targets of miR-338-3p. Thus,  
349 the activation of the *Igf1r/Igf2* autocrine loop observed after the reduction of the level of miR-338-3p  
350 is probably indirect. Interestingly, the inhibition of miR-338-3p has been proposed to play a prominent  
351 role in regulating the proliferation of liver and gastric cancer cells by directly targeting the 3'UTR of  
352 mRNAs encoding oncogenes and cell cycle activators (40,41). Analogous mechanisms may also  
353 contribute to the proliferative effect observed in insulin-secreting cells following the reduction of  
354 AATK or its intronic miRNA.

355 In conclusion, we have identified miR-338-3p and its host gene AATK as candidates for gene-based  
356 therapies or drug targets for approaches aiming at promoting  $\beta$ -cell proliferation and  $\beta$ -cell mass  
357 expansion. Moreover, we have shown that the expression of miR-338-3p and AATK is regulated by  
358 common mechanisms, activates overlapping downstream signaling pathways and has similar  
359 functional impacts on insulin-secreting cells. Whether miR-338-3p and AATK have, redundant,  
360 complementary or synergetic actions in promoting  $\beta$ -cell mass expansion under conditions of  
361 increased insulin needs remains to be determined.

362 **Acknowledgments**

363 We thank Ms Sonia Gattesco for her excellent technical support. This work was supported by the  
364 Swiss National Foundation (to RR), European Foundation for the Study of Diabetes (to RR), Société  
365 Francophone du Diabète (to CJ), the Canadian Institutes of Health Research (to M.P), Ministerio de  
366 Economía y Competitividad, Plan Nacional I+D+I (SAF2011-24698) (to FB) and Generalitat de  
367 Catalunya (2009 SGR-224 and ICREA Academia) (to FB). M.P. holds the Canada Research Chair in  
368 Diabetes and Metabolism.

369 **References**

370

- 371 **1.** Bartel DP. MicroRNAs: target recognition and regulatory functions. *Cell* 2009; 136:215-233
- 372 **2.** Guo H, Ingolia NT, Weissman JS, Bartel DP. Mammalian microRNAs predominantly act to  
373 decrease target mRNA levels. *Nature* 2010; 466:835-840
- 374 **3.** Eliasson L, Esguerra JL. Role of non-coding RNAs in pancreatic beta-cell development and  
375 physiology. *Acta Physiol (Oxf)* 2014; 211:273-284
- 376 **4.** Guay C, Roggli E, Nesca V, Jacovetti C, Regazzi R. Diabetes mellitus, a microRNA-related  
377 disease? *Transl Res* 2011; 157:253-264
- 378 **5.** Rodriguez A, Griffiths-Jones S, Ashurst JL, Bradley A. Identification of mammalian  
379 microRNA host genes and transcription units. *Genome Res* 2004; 14:1902-1910
- 380 **6.** Kim VN, Nam JW. Genomics of microRNA. *Trends Genet* 2006; 22:165-173
- 381 **7.** Li SC, Tang P, Lin WC. Intronic microRNA: discovery and biological implications. *DNA and*  
382 *cell biology* 2007; 26:195-207
- 383 **8.** Baskerville S, Bartel DP. Microarray profiling of microRNAs reveals frequent coexpression  
384 with neighboring miRNAs and host genes. *RNA* 2005; 11:241-247
- 385 **9.** Corcoran DL, Pandit KV, Gordon B, Bhattacharjee A, Kaminski N, Benos PV. Features of  
386 mammalian microRNA promoters emerge from polymerase II chromatin immunoprecipitation  
387 data. *PLoS One* 2009; 4:e5279
- 388 **10.** Jacovetti C, Abderrahmani A, Parnaud G, Jonas JC, Peyot ML, Cornu M, Laybutt R,  
389 Meugnier E, Rome S, Thorens B, Prentki M, Bosco D, Regazzi R. MicroRNAs contribute to  
390 compensatory beta cell expansion during pregnancy and obesity. *J Clin Invest* 2012;  
391 122:3541-3551
- 392 **11.** Barik S. An intronic microRNA silences genes that are functionally antagonistic to its host  
393 gene. *Nucleic Acids Res* 2008; 36:5232-5241
- 394 **12.** Gaozza E, Baker SJ, Vora RK, Reddy EP. AATYK: a novel tyrosine kinase induced during  
395 growth arrest and apoptosis of myeloid cells. *Oncogene* 1997; 15:3127-3135

- 396 **13.** Baker SJ, Sumerson R, Reddy CD, Berrebi AS, Flynn DC, Reddy EP. Characterization of an  
397 alternatively spliced AATYK mRNA: expression pattern of AATYK in the brain and neuronal  
398 cells. *Oncogene* 2001; 20:1015-1021
- 399 **14.** Tomomura M, Hasegawa Y, Hashikawa T, Tomomura A, Yuzaki M, Furuichi T, Yano R.  
400 Differential expression and function of apoptosis-associated tyrosine kinase (AATYK) in the  
401 developing mouse brain. *Brain Res Mol Brain Res* 2003; 112:103-112
- 402 **15.** Tomomura M, Morita N, Yoshikawa F, Konishi A, Akiyama H, Furuichi T, Kamiguchi H.  
403 Structural and functional analysis of the apoptosis-associated tyrosine kinase (AATYK)  
404 family. *Neuroscience* 2007; 148:510-521
- 405 **16.** Raghunath M, Patti R, Bannerman P, Lee CM, Baker S, Sutton LN, Phillips PC, Damodar  
406 Reddy C. A novel kinase, AATYK induces and promotes neuronal differentiation in a human  
407 neuroblastoma (SH-SY5Y) cell line. *Brain Res Mol Brain Res* 2000; 77:151-162
- 408 **17.** Ma S, Rubin BP. Apoptosis-associated tyrosine kinase 1 inhibits growth and migration and  
409 promotes apoptosis in melanoma. *Lab Invest* 2014; 94:430-438
- 410 **18.** Kjørholt C, Akerfeldt MC, Biden TJ, Laybutt DR. Chronic hyperglycemia, independent of  
411 plasma lipid levels, is sufficient for the loss of beta-cell differentiation and secretory function  
412 in the db/db mouse model of diabetes. *Diabetes* 2005; 54:2755-2763
- 413 **19.** Peyot ML, Pepin E, Lamontagne J, Latour MG, Zarrouki B, Lussier R, Pineda M, Jetton TL,  
414 Madiraju SR, Joly E, Prentki M. Beta-cell failure in diet-induced obese mice stratified  
415 according to body weight gain: secretory dysfunction and altered islet lipid metabolism  
416 without steatosis or reduced beta-cell mass. *Diabetes* 2010; 59:2178-2187
- 417 **20.** Gotoh M, Maki T, Satomi S, Porter J, Bonner-Weir S, O'Hara CJ, Monaco AP. Reproducible  
418 high yield of rat islets by stationary in vitro digestion following pancreatic ductal or portal  
419 venous collagenase injection. *Transplantation* 1987; 43:725-730
- 420 **21.** Ayuso E, Mingozzi F, Montane J, Leon X, Anguela XM, Haurigot V, Edmonson SA, Africa  
421 L, Zhou S, High KA, Bosch F, Wright JF. High AAV vector purity results in serotype- and  
422 tissue-independent enhancement of transduction efficiency. *Gene Ther* 2010; 17:503-510

- 423 **22.** Lock M, McGorray S, Auricchio A, Ayuso E, Beecham EJ, Blouin-Tavel V, Bosch F, Bose  
424 M, Byrne BJ, Caton T, Chiorini JA, Chtarto A, Clark KR, Conlon T, Darmon C, Doria M,  
425 Douar A, Flotte TR, Francis JD, Francois A, Giacca M, Korn MT, Korytov I, Leon X, Leuchs  
426 B, Lux G, Melas C, Mizukami H, Moullier P, Muller M, Ozawa K, Philipsberg T, Poulard K,  
427 Raupp C, Riviere C, Roosendaal SD, Samulski RJ, Soltys SM, Surosky R, Tenenbaum L,  
428 Thomas DL, van Montfort B, Veres G, Wright JF, Xu Y, Zeleniaia O, Zentilin L, Snyder RO.  
429 Characterization of a recombinant adeno-associated virus type 2 Reference Standard Material.  
430 Hum Gene Ther 2010; 21:1273-1285
- 431 **23.** Jimenez V, Ayuso E, Mallol C, Agudo J, Casellas A, Obach M, Munoz S, Salavert A, Bosch  
432 F. In vivo genetic engineering of murine pancreatic beta cells mediated by single-stranded  
433 adeno-associated viral vectors of serotypes 6, 8 and 9. Diabetologia 2011; 54:1075-1086
- 434 **24.** Ebert MS, Neilson JR, Sharp PA. MicroRNA sponges: competitive inhibitors of small RNAs  
435 in mammalian cells. Nat Methods 2007; 4:721-726
- 436 **25.** Ebert MS, Sharp PA. MicroRNA sponges: progress and possibilities. RNA 2010; 16:2043-  
437 2050
- 438 **26.** Faustman D, Davis M. TNF receptor 2 pathway: drug target for autoimmune diseases. Nature  
439 reviews Drug discovery 2010; 9:482-493
- 440 **27.** Rieck S, Kaestner KH. Expansion of beta-cell mass in response to pregnancy. Trends  
441 Endocrinol Metab 2010; 21:151-158
- 442 **28.** Terauchi Y, Takamoto I, Kubota N, Matsui J, Suzuki R, Komeda K, Hara A, Toyoda Y, Miwa  
443 I, Aizawa S, Tsutsumi S, Tsubamoto Y, Hashimoto S, Eto K, Nakamura A, Noda M, Tobe K,  
444 Aburatani H, Nagai R, Kadowaki T. Glucokinase and IRS-2 are required for compensatory  
445 beta cell hyperplasia in response to high-fat diet-induced insulin resistance. J Clin Invest 2007;  
446 117:246-257
- 447 **29.** Georgia S, Hinault C, Kawamori D, Hu J, Meyer J, Kanji M, Bhushan A, Kulkarni RN. Cyclin  
448 D2 is essential for the compensatory beta-cell hyperplastic response to insulin resistance in  
449 rodents. Diabetes 2010; 59:987-996

- 450 **30.** Davis DB, Lavine JA, Suhonen JI, Krautkramer KA, Rabaglia ME, Sperger JM, Fernandez  
451 LA, Yandell BS, Keller MP, Wang IM, Schadt EE, Attie AD. FoxM1 is up-regulated by  
452 obesity and stimulates beta-cell proliferation. *Molecular endocrinology* (Baltimore, Md 2010;  
453 24:1822-1834
- 454 **31.** Cornu M, Modi H, Kawamori D, Kulkarni RN, Joffraud M, Thorens B. Glucagon-like  
455 peptide-1 increases beta-cell glucose competence and proliferation by translational induction  
456 of insulin-like growth factor-1 receptor expression. *The Journal of biological chemistry* 2010;  
457 285:10538-10545
- 458 **32.** Cornu M, Yang JY, Jaccard E, Poussin C, Widmann C, Thorens B. Glucagon-like peptide-1  
459 protects beta-cells against apoptosis by increasing the activity of an IGF-2/IGF-1 receptor  
460 autocrine loop. *Diabetes* 2009; 58:1816-1825
- 461 **33.** Griffiths-Jones S, Grocock RJ, van Dongen S, Bateman A, Enright AJ. miRBase: microRNA  
462 sequences, targets and gene nomenclature. *Nucleic Acids Res* 2006; 34:D140-144
- 463 **34.** Osokine I, Hsu R, Loeb GB, McManus MT. Unintentional miRNA ablation is a risk factor in  
464 gene knockout studies: a short report. *PLoS Genet* 2008; 4:e34
- 465 **35.** Buning H, Perabo L, Coutelle O, Quadt-Humme S, Hallek M. Recent developments in adeno-  
466 associated virus vector technology. *J Gene Med* 2008; 10:717-733
- 467 **36.** Filardo EJ, Quinn JA, Frackelton AR, Jr., Bland KI. Estrogen action via the G protein-coupled  
468 receptor, GPR30: stimulation of adenylyl cyclase and cAMP-mediated attenuation of the  
469 epidermal growth factor receptor-to-MAPK signaling axis. *Molecular endocrinology*  
470 (Baltimore, Md 2002; 16:70-84
- 471 **37.** Yu Z, Jin T. New insights into the role of cAMP in the production and function of the incretin  
472 hormone glucagon-like peptide-1 (GLP-1). *Cellular signalling* 2010; 22:1-8
- 473 **38.** Gokey NG, Srinivasan R, Lopez-Anido C, Krueger C, Svaren J. Developmental regulation of  
474 microRNA expression in Schwann cells. *Mol Cell Biol* 2012; 32:558-568
- 475 **39.** Kos A, Olde Loohuis NF, Wieczorek ML, Glennon JC, Martens GJ, Kolk SM, Aschrafi A. A  
476 potential regulatory role for intronic microRNA-338-3p for its host gene encoding apoptosis-  
477 associated tyrosine kinase. *PLoS One* 2012; 7:e31022

- 478 **40.** Li P, Chen X, Su L, Li C, Zhi Q, Yu B, Sheng H, Wang J, Feng R, Cai Q, Li J, Yu Y, Yan M,  
479 Liu B, Zhu Z. Epigenetic silencing of miR-338-3p contributes to tumorigenicity in gastric  
480 cancer by targeting SSX2IP. PLoS One 2013; 8:e66782
- 481 **41.** Fu X, Tan D, Hou Z, Hu Z, Liu G. miR-338-3p Is Down-Regulated by Hepatitis B Virus X  
482 and Inhibits Cell Proliferation by Targeting the 3'-UTR Region of CyclinD1. Int J Mol Sci  
483 2012; 13:8514-8539
- 484

485 **Figure legends**

486

487 **FIGURE 1. Intraductal delivery of AAV8-miR-338-3p sponge promotes  $\beta$ -cell proliferation.** **A,**  
488 Schematic representation of the construct used to specifically block the activity of miR-338-3p in  
489 pancreatic beta-cells. The multimerized binding sites present on the “sponge” selectively sequester  
490 miR-338-3p and prevent its interaction with its endogenous targets. The expression of the sponge is  
491 driven by the rat insulin promoter insuring beta-cell-specific expression of large amounts of the  
492 construct. **B-I,** Mice were injected intraductally with  $1 \times 10^{12}$  viral genomes of AAV8-control sponge or  
493 AAV8-miR-338-3p sponge. Both expression cassettes also encoded the GFP reporter gene and were  
494 driven by the rat insulin promoter. Animals were analyzed 1 month after injection. **B,** Quantification  
495 of transduced islets per pancreas (%). **C,** Quantification of transduced  $\beta$ -cells per islets (%). **D,**  
496 Immunohistochemical analysis of GFP (green) and insulin (red) abundance in islets. Transduced cells  
497 were exclusively  $\beta$ -cells. **E,**  $\beta$ -cell and non  $\beta$ -cell replication was assessed by Ki67 and GFP co-  
498 immunostaining (%). **F,** Image showing examples of double-positive Ki67+/GFP+ islet cells (Ki67  
499 staining in red; GFP+ cells in green; nuclear staining in blue). **G,**  $\beta$ -cell replication assessed by co-  
500 immunostaining with Ki67 and insulin. **H,** Ki67+  $\beta$ -cells, red;  $\beta$ -cells, green; nuclei, blue; arrows  
501 indicate Ki67+  $\beta$ -cells. **I,**  $\beta$ -cell mass was measured after injection of AAV8-control sponge or AAV8-  
502 sponge miR-338-3p in ICR mice by using insulin staining and weighting pancreas (mg). Results are  
503 expressed as mean  $\pm$  SD; n=4-5 animals per group. \*p<0.05 was considered significant versus control.

504

505 **FIGURE 2. AATK expression is reduced in islets of insulin resistant animals.** AATK mRNA  
506 levels were measured by qRT-PCR in islets from pregnant rats at different stages of gestation **A,** 6-  
507 week-old pre-diabetic db/db mice **B,** and diet-induced obese (DIO) mice fed a high-fat-diet for 8  
508 weeks **C.** Data are the mean  $\pm$  SD from 4 animals, normalized by 18S. \*p<0.05 versus control.

509

510 **FIGURE 3. miR-338-3p and AATK expression is reduced in INS832/13 cells treated with a**  
511 **cAMP-raising agent.** miR-338-3p and AATK mRNA levels were measured by qRT-PCR in



512 INS832/13 cells exposed to 1mM IBMX for the indicated periods. Data were normalized by 18S or  
513 U6 levels for mRNAs and miRNAs, respectively. They represent the mean  $\pm$  SD from 3 independent  
514 experiments. \* $p$ <0.05 versus control.

515

516 **FIGURE 4. 17- $\beta$  estradiol and the GLP1-analogue exendin-4 elicit AATK decrease.**

517 AATK expression was measured by qRT-PCR in rat **A, C, D** and human **B, E** islets. **A, B**, Islets were  
518 treated for 48h with 100 nM of 17- $\beta$  estradiol, **C**, 100 nM of the GPR30 agonist G1 or **D, E**, 100 nM  
519 of the GLP1 analogue exendin-4. Data are the mean  $\pm$  SD from 3 independent experiments normalized  
520 by 18S. \* $p$ <0.05 versus control.

521

522 **FIGURE 5. Silencing of AATK and inhibition of miR-338-3p in INS832/13 cells reproduce their**  
523 **decreased levels observed in islets of insulin resistant animal models.** **A**, miR-338-3p expression

524 and AATK mRNA levels were measured by qRT-PCR three days following transfection with siGFP  
525 or siAATK, normalized by U6 or 18S. **B**, AATK protein levels were assessed by western blot 72h  
526 after transfection of siGFP or siAATK and normalized by tubulin. **C**, Western blot quantification. **D**,  
527 INS832/13 cells were transfected with anti-miR-338-3p or with a scrambled sequence single stranded  
528 used as an anti-miR-control. miR-338-3p expression and AATK mRNA levels were measured by  
529 qRT-PCR and normalized to U6 or 18S levels. Results represent the mean  $\pm$  SD from 3-6 independent  
530 experiments. \*  $p$ <0.05 versus control.

531

532 **FIGURE 6. Functional role of AATK and miR-338-3p in INS832/13 cells.** INS832/13 cells were

533 transfected for 72 hours either with anti-miR-338-3p (anti-338-3p), anti-miR-control (anti-ctrl),  
534 siAATK or siGFP as control. **A**, Cell replication was assessed by scoring the Ki67-stained cells.  
535 Insulin secretion. **B**, and insulin content. **C**, in response to 2 mM glucose as basal condition (Black  
536 bars) or 20 mM glucose, 10  $\mu$ M forskolin, 100 $\mu$ M IBMX as a cocktail for stimulatory condition (grey  
537 bars). Insulin release is expressed as percentage of insulin content (IC). **D**, Cells were incubated for 24  
538 hours with (+) or without (-) a mix of proinflammatory cytokines (10 ng/ml TNF- $\alpha$ , 0.1 ng/ml IL-1 $\beta$ ,  
539 30 ng/ml IFN- $\gamma$ ) or **E**, for 48 hours either with 0.5% BSA (-) or with 0.5% BSA coupled to 0.5 mM

540 palmitate (+). **D, E**, Apoptosis was assessed by staining the cells with Hoechst and counting the  
541 picnotic nuclei. **F**, Birc5, Foxm1, Cyclin D2, Igf1r, Irs2, Bcl2, Bcl-xl, and Bad expression were  
542 measured by qRT-PCR and compared with the level in cells transfected with a scrambled antimiR or  
543 siGFP as controls. Data are expressed as fold changes. Data are expressed as mean  $\pm$  SD from 3-5  
544 independent experiments. \*, # p<0.05.

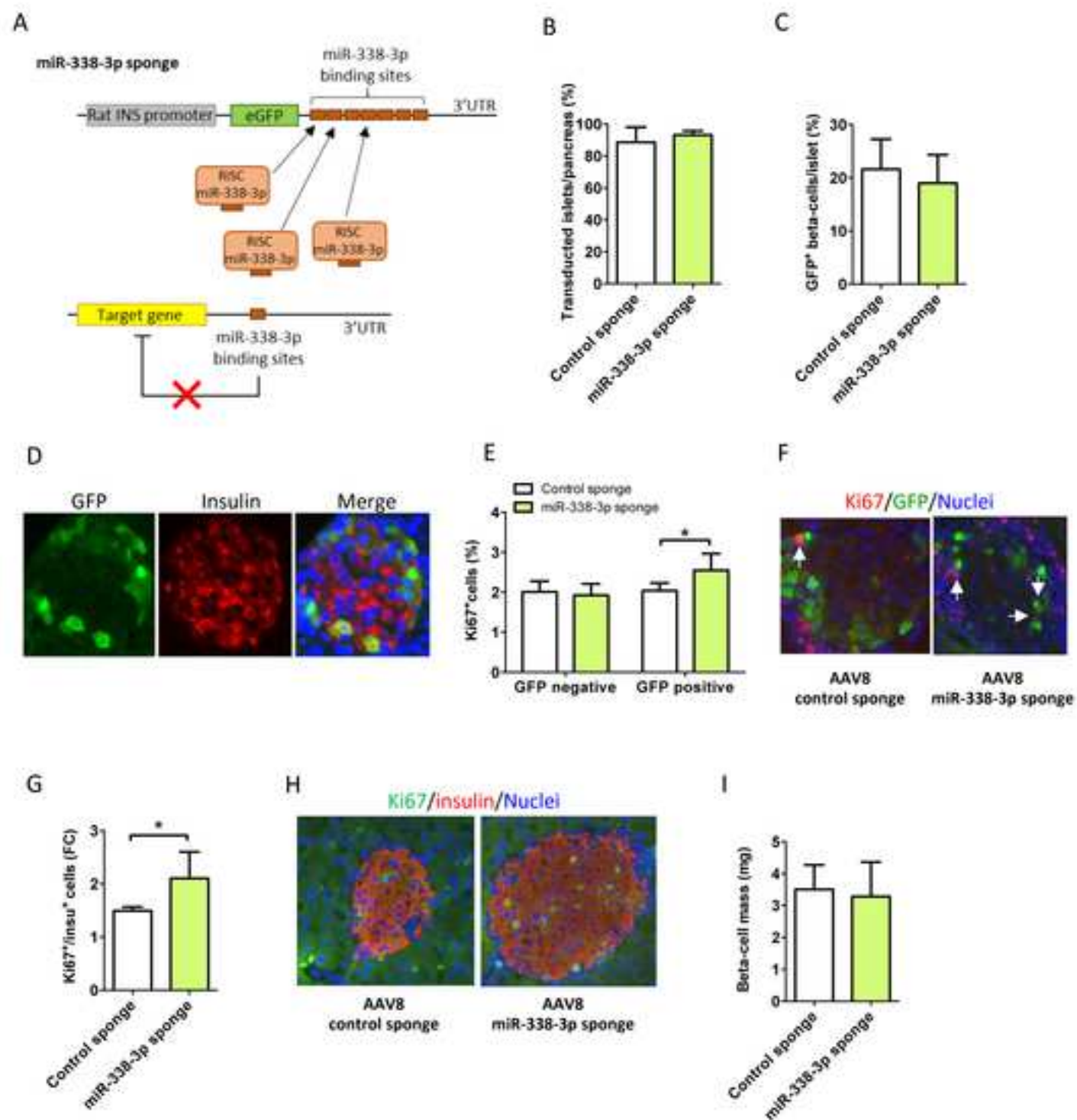
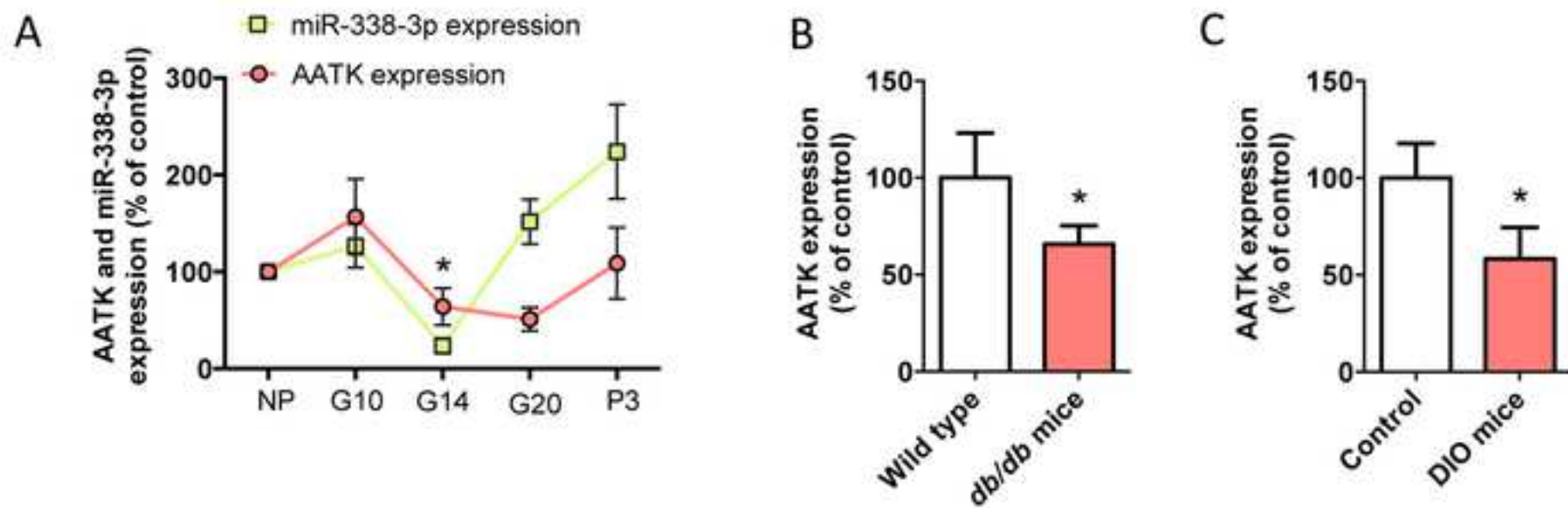
Figure 1. *Jacovetti et al.*

Figure 2. *Jacovetti et al.*

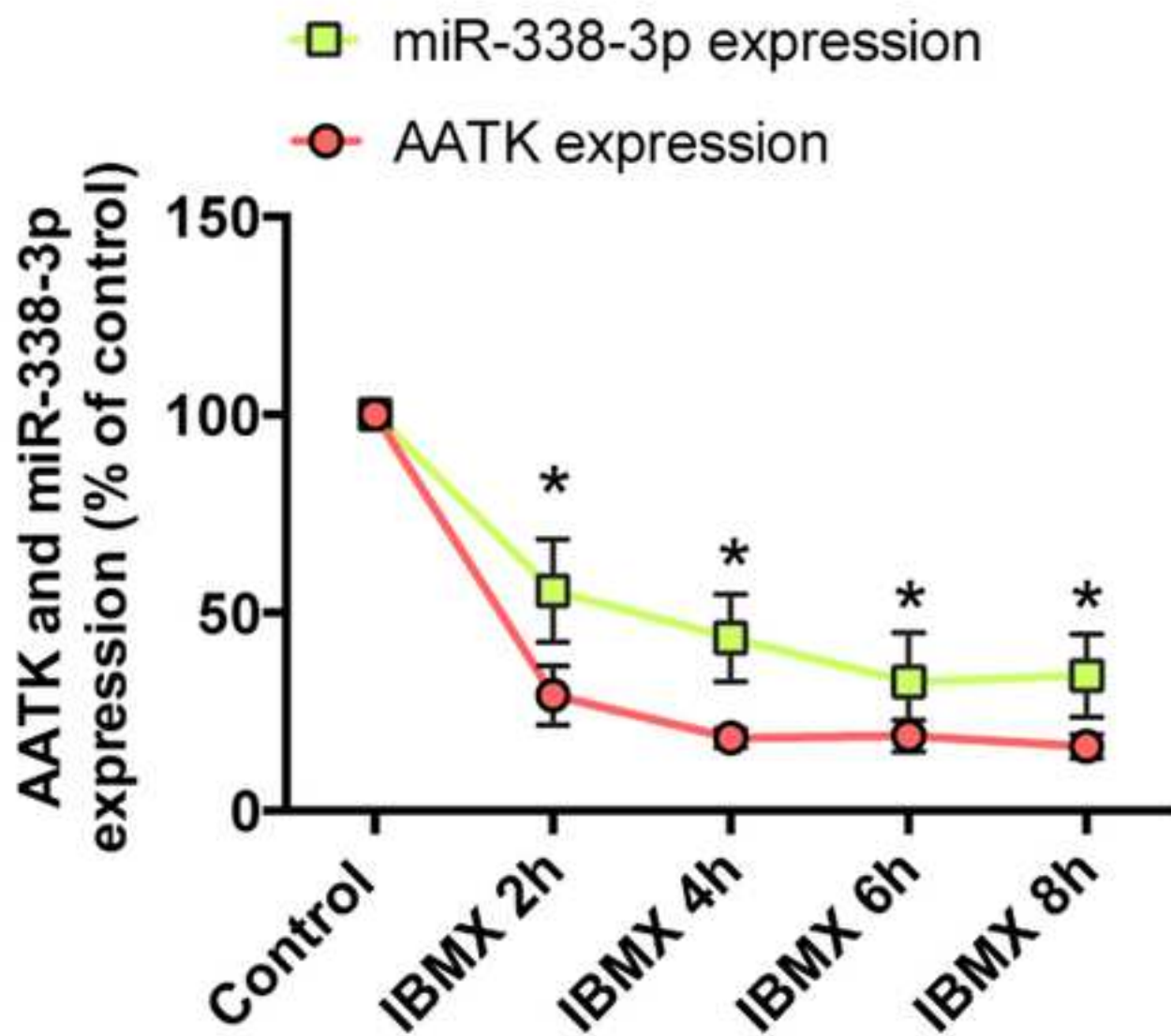
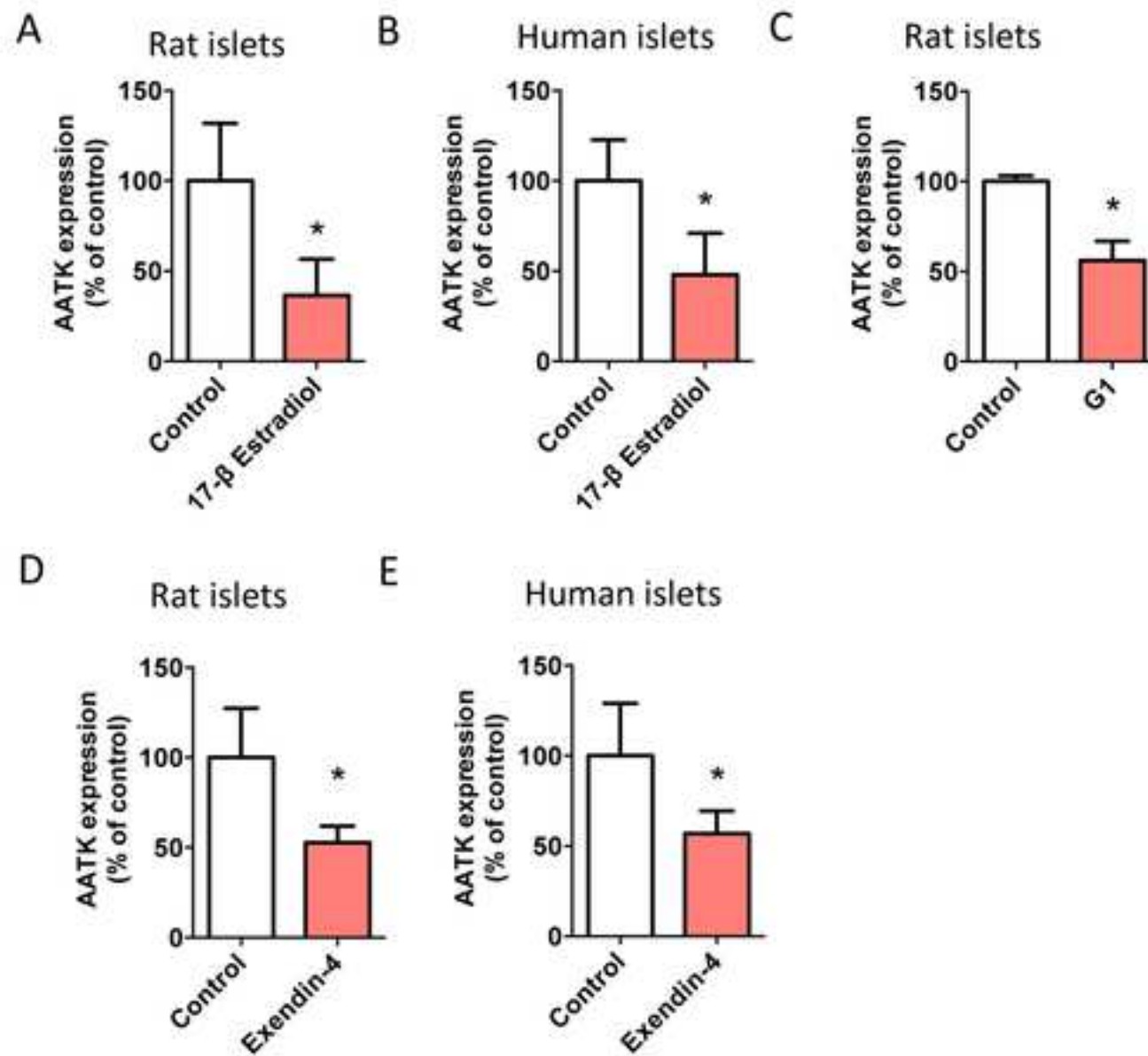
*Figure 3. Jacovetti et al.*

Figure 4. *Jacovetti et al.*



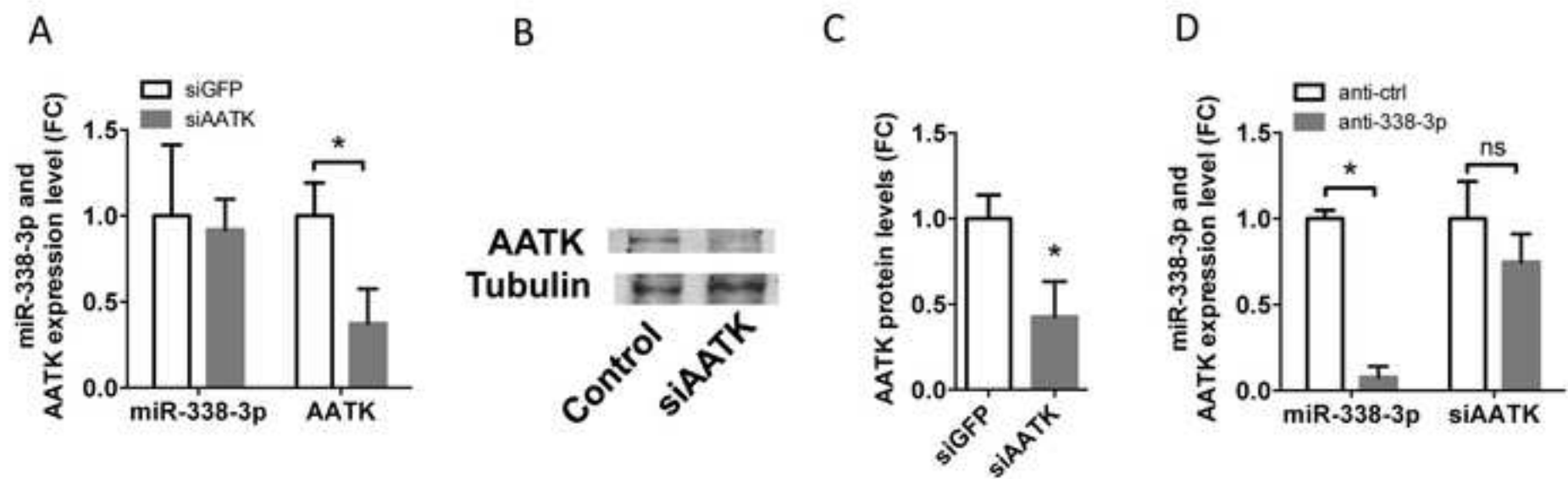
*Figure 5. Jacovetti et al.*

Figure 6. *Jacovetti et al.*

